Direct Time-Resolved Study of the Gas-Phase Reactions of Germylene with Ethyl- and Diethylgermane: Absolute Rate Constants, Temperature Dependences, and Mechanism

Rosa Becerra

Instituto de Quimica-Fisica "Rocasolano", CSIC, C/Serrano 119, 28006 Madrid, Spain

Sergey E. Boganov, Mikhail P. Egorov, Irina V. Krylova, and Oleg M. Nefedov

N.D. Zelinsky Institute of Organic Chemistry, Russian Academy of Sciences, Leninsky Prospekt 47, 117913 Moscow, Russian Federation

Robin Walsh*

Department of Chemistry, University of Reading, Whiteknights, P. O. Box 224, Reading, RG6 6AD, U.K.

Received: September 21, 2006; In Final Form: December 11, 2006

Time-resolved studies of germylene, GeH_2, generated by the 193 nm laser flash photolysis of 3,4-dimethyl-1-germacyclopent-3-ene, have been carried out to obtain rate constants for its bimolecular reactions with ethyl- and diethylgermanes in the gas phase. The reactions were studied over the pressure range 1−100 Torr with SF_6 as bath gas and at five temperatures in the range 297−564 K. Only slight pressure dependences were found for $GeH_2 + EtGeH_3$ (399, 486, and 564 K). The high pressure rate constants gave the following Arrhenius parameters: for $GeH_2 + EtGeH_3$, $\log A = -10.75 \pm 0.08$ and $E_a = -6.7 \pm 0.6$ kJ mol^{-1}; for $GeH_2 + Et_2GeH_2$, $\log A = -10.68 \pm 0.11$ and $E_a = -6.95 \pm 0.80$ kJ mol^{-1}. These are consistent with fast, near collision-controlled, association processes at 298 K. RRKM modeling calculations are, for the most part, consistent with the observed pressure dependence of $GeH_2 + EtGeH_3$. The ethyl substituent effects have been extracted from these results and are much larger than the analogous methyl substituent effects in the SiH_2 + methylsilane reaction series. This is consistent with a mechanistic model for Ge−H insertion in which the intermediate complex has a sizable secondary barrier to rearrangement.

Introduction

The reactions of germylene, GeH_2, are of interest both because of their involvement in the breakdown mechanisms of germanes leading to solid germanium (chemical vapor deposition)[1,2] and also because of their participation in germane[3] and organogermane decompositions.[4] In 1996 we reported the first directly measured rate constants for GeH_2 reactions[5] carried out by time-resolved means in the gas phase. Since then we have undertaken a series of gas-phase studies of the kinetics of GeH_2 in order to throw light onto the mechanisms of its various reactions.[6−15] The group of King and Lawrance have also begun similar studies.[16−18] Among the principal reactions of interest are the insertion processes of GeH_2 into Ge−H bonds[6,7,11,15−17] and Si−H bonds[8,10,16,17] which have been shown to proceed via association complexes rather similar to those implicated in the insertion reactions of SiH_2.[19−25] The results show that, although they are quite fast under the conditions of study, GeH_2 reactions occur more slowly than their SiH_2 counterparts.

Among useful probes of reactivity are substituent effects. In studies of SiH_2 with the methylsilanes Baggott et al.[21] and Becerra et al.[26] have found, inter alia, that at 298 K SiH_2 reacts more slowly with Me_3SiH than with SiH_4 (although the *per Si−H bond* reactivities were the other way round). For GeH_2, by contrast, the reaction with Et_3GeH[6] is faster than that with GeH_4[7] both overall and per Ge−H bond. The reaction of $GeH_2 + Et_3GeH$ also has a more negative activation energy than that of $SiH_2 + Me_3SiH$. It is assumed here that the differences between Et and Me substitution are not significant. To understand these effects more fully, we decided to investigate the further insertion reactions of GeH_2 with $EtGeH_3$ and Et_2GeH_2. This enables us to make the complete comparison of reactions 1−4.

$$GeH_2 + GeH_4 \rightarrow Ge_2H_6 \quad (1)$$

$$GeH_2 + EtGeH_3 \rightarrow EtGeH_2GeH_3 \quad (2)$$

$$GeH_2 + Et_2GeH_2 \rightarrow Et_2GeHGeH_3 \quad (3)$$

$$GeH_2 + Et_3GeH \rightarrow Et_3GeGeH_3 \quad (4)$$

Reactions 2 and 3 have not previously been studied. The ethylgermanes were selected here (rather than the methylgermanes) simply for comparison purposes. Originally,[6] Et_3GeH was chosen as a substrate rather than Me_3GeH, because of its more ready availability.

Experimental Section

Germylene kinetic studies have been carried out by the laser flash photolysis/laser absorption technique, details of which have been published previously.[5,7] Only essential and brief details are therefore included here. GeH_2 was produced by the 193 nm flash photolysis of 3,4-dimethyl-1-germacyclopent-3-ene (DMGCP) by use of a Lamba Physik (Coherent) Compex 100 excimer laser. GeH_2 concentrations were monitored in real time by means of a Coherent 699-21 single-mode dye laser

10.1021/jp0661948 CCC: $37.00
Published on Web 02/06/2007

pumped by an Innova 90-5 argon ion laser and operating with Rhodamine 6G. Experiments were carried out in a variable temperature spectrosil quartz vessel with demountable windows which were regularly cleaned. Photolysis laser pulse energies were typically 50−70 mJ with a variation of ±5%. The monitoring laser beam was multipassed 32 times through the reaction zone to give an effective path length of ca. 1.0 m. The laser wavelength was set by the combined use of a wavemeter (Burleigh WA-20) and reference to a known coincident transition in the visible spectrum of I_2 vapor and was checked at frequent intervals during the experiments.

The monitoring laser was tuned to 17 111.31 cm^{-1} corresponding to a known strong vibration−rotation transition ($\tilde{A}^1B_1$-(0,1,0) ← $\tilde{X}^1A_1$(0,0,0) band) discovered by us previously,[5] and now assigned as the $^pQ_1(6)$ line by intracavity laser absorption spectroscopy by Campargue and Escribano.[27] Light signals were measured by a dual photodiode/differential amplifier combination, and signal decays were stored in a transient recorder (Datalab DL 910) interfaced to a BBC microcomputer. This was used to average the decays of typically five laser shots (at a repetition rate of 1 or 0.5 Hz). Signal decays were found to be exponential up to 90% and were fitted by a nonlinear-least-squares procedure to provide values for the first-order rate coefficients, k_{obs}, for removal of GeH_2 in the presence of known partial pressures of substrate, either $EtGeH_3$ or Et_2GeH_2.

The gas mixtures for photolysis were made up consisting of 2.5−9 mTorr DMGCP, variable pressures of substrate between 4.5 and 220 mTorr, and inert diluent bath gas, SF_6, up to total pressures between 1 and 100 Torr, although most experiments were done at 10 Torr. Pressures were measured with capacitance manometers (MKS Baratron).

DMGCP was prepared as previously described.[5] $EtGeH_3$ and Et_2GeH_2 were prepared by $LiAlH_4$ reduction of $EtGeCl_3$ and Et_2GeBr_2, respectively, in dried *n*-Bu_2O by standard procedures.[28a] $EtGeCl_3$ was made by direct synthesis from Ge and EtCl.[28b] Et_2GeBr_2 was prepared from Et_4Ge according to the procedure of Mironov and Kravchenko.[29] Et_4Ge was made by the Grignard method.[30] The ethylgermanes were purified by low pressure distillation, and characterized by IR and NMR spectroscopies. Final purities, based on gas chromatographic (GC) analysis (2 m silicone oil column (OV101), Perkin-Elmer 8310 chromatograph operated at ambient temperature), were 98.2% ($EtGeH_3$) and 99.6% (Et_2GeH_2). SF_6 was obtained from ICI and contained no GC detectable impurities.

The OV101 GC column, operated at 60 °C, was also used for product analytical studies. The retention times (in minutes) of compounds used or identified in this work under these conditions are as follows: $EtGeH_3$, 1.15; Et_2GeH_2, 2.60; 2,3-dimethyl-1,3-butadiene (DMB), 2.68; $EtGeH_2GeH_3$, 3.26; $Et_2GeHGeH_3$, 10.8; DMGCP, 16.3.

Results

General Considerations. Prior to kinetic studies, checks were made of the UV absorption spectra of $EtGeH_3$ and Et_2GeH_2 at room temperature. $EtGeH_3$ showed no absorption at 193 nm (cross section $< 8 \times 10^{-20}$ cm^2), while Et_2GeH_2 had a small absorption (cross section $= 4.3 \times 10^{-19}$ cm^2). This shows that under experimental conditions (at 298 K) absorption of the excimer laser pulse by the substrates either does not occur or is negligible. For Et_2GeH_2, the calculated absorbance at 193 nm in the reaction vessel at the highest partial pressure (30 mTorr) was 0.0007. It is possible that increased absorption (due to peak broadening) could occur at higher temperatures, but we have no evidence of this.

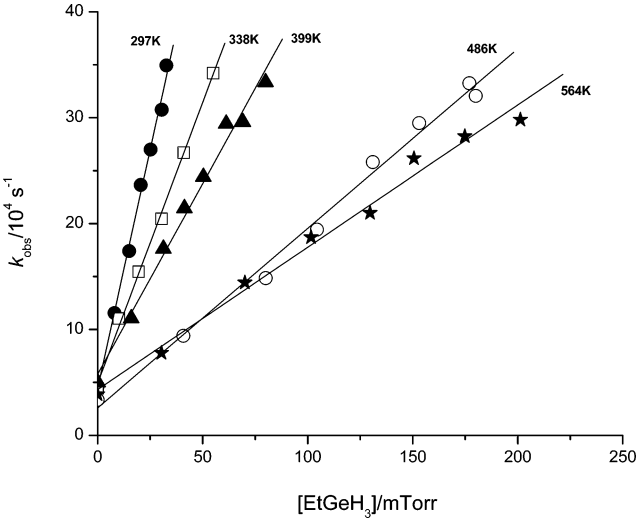

Figure 1. Second-order plots for reaction of GeH_2 + $EtGeH_3$ at 10 Torr (SF_6) at different temperatures (indicated).

For each reaction it was independently verified during preliminary experiments that, in a given reaction mixture, k_{obs} values were not dependent on the exciplex laser energy or number of photolysis shots. Because static gas mixtures were used, tests with up to 20 shots were carried out. The constancy of k_{obs} (five-shot averages) showed no effective depletion of reactants in any of the systems. The sensitivity of detection of GeH_2 was high but decreased with increasing temperature. Therefore, increasing quantities of precursor were required at higher temperatures. However, at any given temperature precursor pressures were kept fixed to ensure a constant (but always small) contribution to k_{obs} values.

For each substrate a series of experiments was carried out at each of five temperatures in the range from room temperature up to ca. 564 K. At 10 Torr total pressure (SF_6 diluent), a number of runs (usually five or more) at different substrate partial pressures were carried out at each temperature. The purpose of these experiments was to establish the second-order nature of the kinetics. In addition to these experiments, another set of runs was carried out at each temperature, in which the total pressure (SF_6) was varied in the range 1−100 Torr to test the pressure dependence of the second-order rate constants. In these runs the number of data points obtained was limited to two or three, but second-order behavior was assumed, and the constants were calculated by assuming a linear dependence of k_{obs} on substrate pressure. To keep errors to a minimum, sufficient substrate was used to ensure k_{obs} values in the range $(2-3) \times 10^5$ s^{-1} where reaction with substrate was at least 75% of the total reaction. Allowance was made for reaction of GeH_2 with precursor (measured directly for each total pressure but found to be pressure independent). The total pressure range investigated was determined by practical considerations. Below 1 Torr, decay traces tended to be noisy, and above 100 Torr, GeH_2 signals were rather small. (Although the reason for this is unknown, it is probably due to quenching of the precursor excited state.) The results of the work described here represent measurements of some 140 decay constants (k_{obs} values) overall. Analysis of the decay constants in the absence of substrate gave rate constants for GeH_2 + DMGCP in the range $(2-6) \times 10^{-10}$ cm^3 $molecule^{-1}$ s^{-1} (generally decreasing with temperature). Bearing in mind that these values are based on only one DMGCP pressure at each temperature, they are in reasonable agreement with the value of 3.5×10^{-10} cm^3 $molecule^{-1}$ s^{-1} obtained earlier at 295 K.[5]

TABLE 1: Experimental Second-Order Rate Constants[a,b] for $GeH_2 + EtGeH_3$ at Various Pressures (SF_6)

	P/Torr				
T/K	1	3	10	30	100
297	2.4 ± 0.2	2.7 ± 0.3	2.76 ± 0.07	2.7 ± 0.3	
338	1.45 ± 0.04	1.79 ± 0.02	1.83 ± 0.03		
399	1.13 ± 0.03	1.58 ± 0.16	1.50 ± 0.05	1.64 ± 0.16	1.82 ± 0.18
486	0.514 ± 0.044	0.755 ± 0.061	0.844 ± 0.025	0.910 ± 0.09	1.01 ± 0.10
564	0.295 ± 0.016	0.441 ± 0.030	0.793 ± 0.025		0.87 ± 0.09

[a] Units: 10^{-10} cm^3 $molecule^{-1}$ s^{-1}. [b] Errors are single standard deviations (10 Torr values) or 10% at most other pressures (see text).

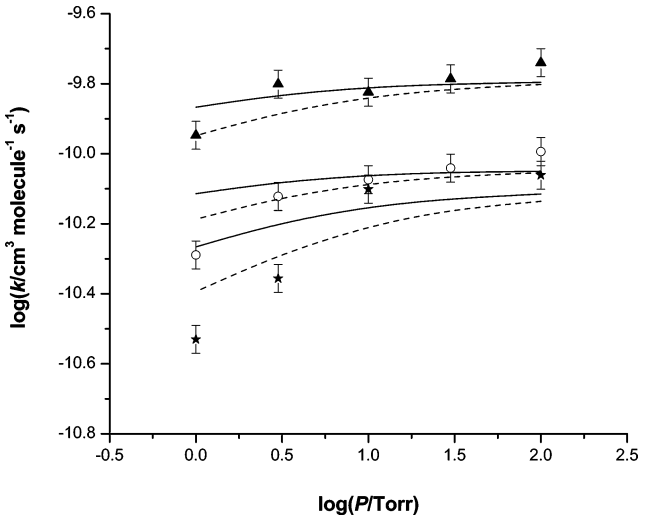

Figure 2. Pressure dependences of rate constants for $GeH_2 + EtGeH_3$ (▲, 399 K; ○, 486 K; ★, 564 K). Lines are RRKM fits at the three temperatures [RRKM(1), —; RRKM(2), ---].

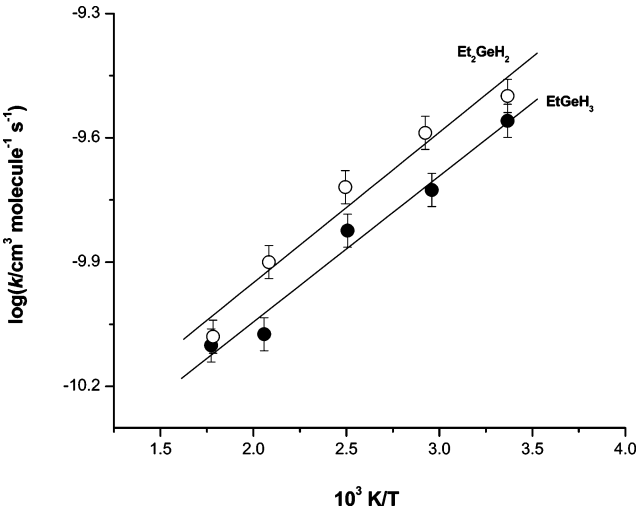

Figure 3. Arrhenius plots for rate constants for $GeH_2 + EtGeH_3$ (●) and $GeH_2 + Et_2GeH_2$ (○). $P = 10$ Torr (SF_6).

Kinetics of $GeH_2 + EtGeH_3$. This reaction was investigated over the temperature range 297−564 K. The second-order rate plots at 10 Torr total pressure are shown in Figure 1 for the five temperatures studied. As can be seen, reasonably linear plots resulted and the second-order rate constants, obtained by least-squares fitting, are collected in Table 1. The error limits are single standard deviations. These are random errors: systematic errors are harder to assess, but based on previous experience we do not anticipate that they should be more than ±10%. The rate constants clearly decrease with increasing temperature.

The pressure dependence of these rate constants was also investigated, and the results are also shown in Table 1. Because the rate constants at other pressures are mostly based on fewer data points, we have assumed uncertainties of ±10% in values to cover both random and systematic errors. At the two lower temperatures the results suggest little or no pressure dependence, except possibly at 1 Torr. At 399 K variations in values are still slight. Only at 486 and 564 K are there more significant signs of falloff at lower pressures. The data are plotted in Figure 2, where they are compared with RRKM theoretical predictions (see next section). This is a much less marked pressure dependence than that for the reaction of $GeH_2 + GeH_4$ (found by us earlier[7]). Because the theory suggested very little pressure dependence, infinite pressure values were taken to be the same as those obtained at 10 Torr. An Arrhenius plot of k_2 values, shown in Figure 3, gives a reasonably linear fit, bearing in mind the uncertainties. The resulting Arrhenius equation is

$$\log(k_2/\mathrm{cm^3\ molecule^{-1}\ s^{-1}}) = (-10.75 \pm 0.08) + (6.74 \pm 0.61)\ \mathrm{kJ\ mol^{-1}}/(RT\ \ln 10)$$

If the theoretical values of k_2^∞ are taken at 399, 486, and 564 K, then the resulting equation is

$$\log(k_2^\infty/\mathrm{cm^3\ molecule^{-1}\ s^{-1}}) = (-10.73 \pm 0.09) + (6.65 \pm 0.65)\ \mathrm{kJ\ mol^{-1}}/(RT\ \ln 10)$$

Kinetics of $GeH_2 + Et_2GeH_2$. This reaction was investigated over the temperature range 297−561 K. The second-order rate plots at 10 Torr total pressure are shown in Figure 4 for the five temperatures studied. As can be seen, reasonably linear plots resulted and the second-order rate constants, obtained by least-squares fitting, are collected in Table 2. The error limits are single standard deviations. The rate constants clearly decrease with increasing temperature.

This reaction showed negligible pressure dependence. The rate constants found at other pressures were within experimental error the same as those obtained at 10 Torr, even at the highest temperature. Infinite pressure values can safely be assumed to be the same as those at 10 Torr. An Arrhenius plot of k_3 values, also shown in Figure 3, gives a reasonably linear fit, bearing in mind the uncertainties. The resulting Arrhenius equation is

$$\log(k_3/\mathrm{cm^3\ molecule^{-1}\ s^{-1}}) = (-10.68 \pm 0.11) + (6.95 \pm 0.80)\ \mathrm{kJ\ mol^{-1}}/(RT\ \ln 10)$$

End Product Analyses. *(i) $GeH_2 + EtGeH_3$.* A mixture of 0.42 Torr DMGCP and 1.27 Torr $EtGeH_3$ was subjected to 100 shots of 193 nm laser radiation (60 mJ/pulse) and then analyzed by GC. Under these conditions two major product peaks were observed, comprising 93% of the total products based on peak area (at a conversion of ca. 50% of DMGCP). The largest peak (71%) eluted at 2.68 min, and was readily identified as 2,3-

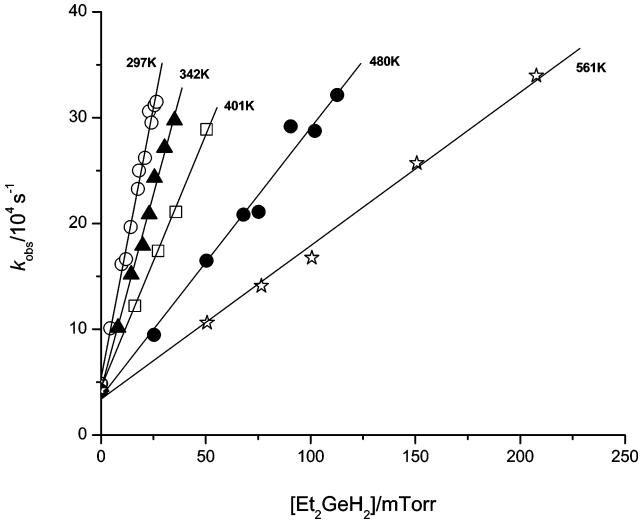

Figure 4. Second-order plots for reaction of $GeH_2 + Et_2GeH_2$ at 10 Torr (SF_6) at different temperatures (indicated).

TABLE 2: Experimental Second-Order Rate Constants[a] for $GeH_2 + Et_2GeH_2$ at 10 Torr (SF_6)

T/K	$k/10^{-10}$ cm^3 molecule^{-1} s^{-1}
297	3.17 ± 0.08
342	2.58 ± 0.08
401	1.91 ± 0.06
480	1.26 ± 0.05
561	0.831 ± 0.025

[a] Errors are single standard deviations.

dimethylbuta-1,3-diene (DMB), the known photodecomposition product of DMGCP.[5] The other major peak (16%), eluting slightly after DMB at 3.26 min, was identified as ethyldigermane as follows (see also the Discussion). A mixture of 0.98 Torr $EtGeH_3$ and 2.04 Torr GeH_4 was photolyzed in the presence of a drop of Hg using 253.7 nm radiation (Hg resonance lamp) for ca. 5 min. When analyzed, the product mixture contained a GC peak with the same retention time (3.26 min) as that seen in the first experiment (above). This peak (42% of the total products based on peak area) was absent in a blank photolysis of Hg*−$EtGeH_3$.

(ii) $GeH_2 + Et_2GeH_2$. A mixture of 0.46 Torr DMGCP and 1.32 Torr Et_2GeH_2 was subjected to 100 shots of 193 nm laser radiation (60 mJ/pulse) and then analyzed by GC. Under these conditions several new product peaks were observed, only one of them substantial. The DMB peak (from DMGCP photodecomposition) coeluted with that of Et_2GeH_2, but the large new peak (85% of the remaining products based on peak area), eluting at 10.8 min, was identified as 1,1-diethyldigermane as follows (see also the Discussion). A mixture of 0.89 Torr Et_2GeH_2 and 2.89 Torr GeH_4 was photolyzed in the presence of a drop of Hg using 253.7 nm radiation (Hg resonance lamp) for ca. 5 min. When analyzed, the product mixture contained a GC peak with the same retention time (10.8 min) as that seen in the first experiment (above). This peak (11% of total products based on peak area) was absent in a blank photolysis of Hg*−Et_2GeH_2. It was also confirmed that no products were formed from the 193 nm laser photolysis of Et_2GeH_2 alone (at 298 K).

RRKM Calculations. Because the $GeH_2 + EtGeH_3$ reaction shows signs of pressure dependence characteristic of a third-body assisted association reaction,[31] as found previously for reaction 1,[7] we undertook RRKM calculations to model this. This was carried out on the reverse reaction −2, viz. the unimolecular decomposition of ethyldigermane, $EtGeH_2GeH_3$, because the pressure dependences of association and dissociation reactions are the same,[31] provided there are no other reaction channels. To our knowledge there has been no kinetic study of the decomposition of $EtGeH_2GeH_3$, and so the necessary parameters for the calculation were estimated. It has been assumed also that the potential side channel leading to EtGeH and GeH_4 is minor, on the basis of analogy with the known decomposition pathways of $MeSiH_2SiH_3$.[32] The following Arrhenius parameters were assumed based on those for Ge_2H_6[7] but with correction for path degeneracy: $\log(A_{-2}/s^{-1}) = 14.42$ and $E_a(-2) = 154.8$ kJ mol^{-1}. It is not possible to state with complete certainty how reliable these parameters are, but on the basis of the similarity of Arrhenius parameters for the decompositions of the structurally similar methyldisilanes[33] (four compounds), it is reasonable to assume that the *A* factor is reliable within a factor of 2 and the activation energy within ±8.4 kJ mol^{-1}.

TABLE 3: Molecular and Transition State Parameters for RRKM Calculation for Ethyldigermane Decomposition at 564 K

	ethyldigermane	ethyldigermane‡
$\tilde{\nu}$/cm^{-1}	2960(5)	2960(5)
	2110(5)	2110(4)
	1450(3)	1500(1)
	1260(2)	1450(3)
	1000(1)	1260(2)
	880(3)	1000(1)
	850(3)	880(2)
	760(2)	850(3)
	700(1)	760(1)
	650(1)	700(1)
	410(4)	650(1)
	350(1)	590(1)
	250(1)	500(1)
	180(1)	410(2)
	170(1)	250(1)
	140(1)	197(1)
	100(1)	190(1)
		180(1)
		170(1)
		140(1)
		100(1)
reaction coordinate/cm^{-1}	350	
path degeneracy	3	
E_o(critical energy)/kJ mol^{-1}	154.8	
$Z_{LJ}/10^{-10}$ cm^3 molecule^{-1} s^{-1}	4.48	

The next stage was to assign the vibrational wavenumbers of the molecule and its activated complex (transition state) at the key temperatures of study. This was done for $EtGeH_2GeH_3$ using group frequencies based on those for Ge_2H_6[34] and those of the C_2H_5 group.[35] The activated complexes were assigned by adjusting the wavenumbers of the key transitional modes, principally those of the GeH_3 group, until a match was obtained with the entropy of activation and the *A* factor in the usual way.[31] Whether precise values of all vibrational wavenumbers are correct or not is not important provided the entropies of activation are matched. The values of the molecular and transition state parameters are shown in Table 3 for the assignment at 564 K, the highest calculation temperature. The table also includes the value of the Lennard-Jones collision number, Z_{LJ} (in SF_6), calculated using the formulas recommended by Troe[36] using the following collision parameters: for SF_6, $\sigma = 5.13$ Å and $\epsilon/k = 222$ K; for $EtGe_2H_5$, $\sigma = 5.61$ Å and $\epsilon/k = 463$ K. These were obtained or estimated from those for similar molecules listed by Reid et al.[37] Small changes (not shown) were made to the $EtGeH_2GeH_3$ activated complex wavenumbers and Z_{LJ} values for the RRKM calculations at 486

and 399 K. We have assumed that geometry changes in the decomposing $EtGeH_2GeH_3$ molecule do not lead to significant changes in overall moments of inertia and abiabatic rotational effects. This is an approximation, in view of the loose activated complex structures, but we believe it will not lead to serious errors. However, we have used a weak collisional (stepladder) model for collisional deactivation,[31] because there is overwhelming evidence against the strong collision assumption.[38] The average energy removal parameter, $\langle\Delta E\rangle_{down}$, was taken as 9.6 kJ mol^{-1} (800 cm^{-1}) for all reactions by analogy with earlier studies[7,12] of GeH_2 reactions, although variations within the range 8.4−12.0 kJ mol^{-1} had little effect on the fitting. The results of these calculations, called RRKM(1), are shown graphically in Figure 2, where they are compared with experiment. Because the trends of these calculations were somewhat less than those observed, we extended these calculations within the possible uncertainties in the values of A and E_o for decomposition (see above). Another set of calculations, called RRKM(2), was based on values of $\log(A_{-2}/s^{-1}) = 14.72$ and $E_a(-2) = 146.4$ kJ mol^{-1}. All these results are discussed below.

Discussion

Product Identification and Overall Reactions. The identification of the unknown GC peaks was made by the following argument. The technique of mercury (6^3P_1) photosensitization is known to proceed via X−H bond cleavage.[39] The mechanism for reaction in mixtures of $EtGeH_3 + GeH_4$ should be as follows:

$$Hg^* + GeH_4 \rightarrow GeH_3 + H + Hg$$

$$Hg^* + EtGeH_3 \rightarrow EtGeH_2 + H + Hg$$

$$H + GeH_4 \rightarrow GeH_3 + H_2$$

$$H + EtGeH_3 \rightarrow EtGeH_2 + H_2$$

$$2GeH_3 \rightarrow Ge_2H_6$$

$$GeH_3 + EtGeH_2 \rightarrow EtGeH_2GeH_3$$

$$2EtGeH_2 \rightarrow EtGeH_2GeH_2Et$$

Of the expected end products, Ge_2H_6 does not give a GC signal (using FID)[8] and $EtGeH_2GeH_2Et$ was not seen, probably because GeH_4 was used in a 2-fold excess, leaving only $EtGeH_2GeH_3$, which corresponded to the product of the $GeH_2 + EtGeH_3$ study. Exactly similar and parallel arguments establish $Et_2GeHGeH_3$ as the product of the $GeH_2 + Et_2GeH_2$ reaction. These results confirm the formation of the expected products based on earlier studies of GeH_2 insertion into Ge−H bonds.[40−42] This approach was used previously to identify Me_3SiGeH_3 as the product of $GeH_2 + Me_3SiH$.[8]

RRKM Calculations and Pressure Dependence. The experimental measurements of extent of pressure dependence and calculated degrees of falloff for reaction 2, that of $GeH_2 + EtGeH_3$, are compared in Figure 2. The results of the first set of calculations, RRKM(1), are in reasonable agreement with experiment at all pressures except 1 Torr at 399 and 486 K. At 564 K the agreement is less good. However, the calculations do support the conclusion that at pressures of 10 Torr and above the reaction is close to its high pressure limit. The calculations RRKM(2) correspond to a slightly looser transition state with a slightly lower critical energy, within the reasonable uncertainty range of our estimates of these parameters. The increased curvature in the plots reflects somewhat better the trends in the data at all temperatures, although the fit at 564 K is still not good. However, the problem with RRKM(2) is that at 10 Torr at 564 K the rate constant is predicted to be 20% below the high pressure limit. This cannot be ruled out given the scatter of the data. This indicates that loosening the transition state in these calculations does help with the fit. However, we still suspect that there may be a systematic source of error in the measurements at the low pressures, which we were unable to pinpoint. Despite this, we believe, on the basis of the large majority of measurements, that the data are reliable and, from the RRKM calculations, that the reaction has very little pressure dependence. Use of k_2 (10 Torr) or k_2^∞ in the Arrhenius plots makes very little difference, although k_2^∞ would be better if there were less scatter in the data at 564 K.

TABLE 4: Comparison of Arrhenius Parameters for Ge−H Insertion Reactions of GeH_2

reaction	log A^a	E_a/kJ mol^{-1}	ref
$GeH_2 + GeH_4$	-11.17 ± 0.10^b	-5.2 ± 0.7^b	7
$GeH_2 + EtGeH_3$	-10.75 ± 0.08	-6.7 ± 0.6	this work
$GeH_2 + Et_2GeH_2$	-10.68 ± 0.11	-6.95 ± 0.80	this work
$GeH_2 + Et_3GeH$	-11.43 ± 0.15	-10.6 ± 1.1	6

[a] Units: cm^3 molecule^{-1} s^{-1}. [b] High pressure limiting values.

TABLE 5: Comparison of Room-Temperature Rate Constants[a] for Ge−H Insertion Reactions of GeH_2

reaction	$10^{10}k$(298 K)^{a,b}	k_{rel}	k_{rel}(per Ge-H)
$GeH_2 + GeH_4$	0.547[c]	1	1.0
$GeH_2 + EtGeH_3$	2.70	4.94	6.6
$GeH_2 + Et_2GeH_2$	3.45	6.31	12.6
$GeH_2 + Et_3GeH$	2.72	4.97	19.9

[a] Units: 10^{-10} cm^3 molecule^{-1} s^{-1}. [b] Values calculated from Arrhenius equations. [c] High pressure limiting value.

TABLE 6: Comparison of Room-Temperature Rate Constants[a,b] for Si−H Insertion Reactions of SiH_2

reaction	$10^{10}k$(298 K)^a	k_{rel}	k_{rel}(per Si-H)
$SiH_2 + SiH_4$	4.6[c]	1	1.0
$SiH_2 + MeSiH_3$	4.1	0.89	1.2
$SiH_2 + MeSiH_2$	3.5	0.76	1.5
$SiH_2 + Me_3SiH$	2.5	0.54	2.2

[a] Units: 10^{-10} cm^3 molecule^{-1} s^{-1}. [b] From ref 26. [c] High pressure limiting value.

Rate Constant Comparisons. To our knowledge, these are the first measurements of gas-phase rate constants for reactions 2 and 3. The measured Arrhenius parameters are compared with those of reactions 1 and 4 in Table 4. The values are very comparable for all these reactions with A factors in the range $10^{-11.0\pm0.4}$ cm^3 molecule^{-1} s^{-1} and negative activation energies between −5 and −11 kJ mol^{-1}. Although the A factors show no systematic trend, there is a trend toward more negative activation energies with increasing ethyl group substitution. To gain further insight into these reactions, we have singled out the rate constants at 298 K for comparison. These are shown in Table 5. The rate constants for reactions 2−4 are significantly larger than that for reaction 1, showing that the effect of ethyl substitution in the substrate germane is to increase markedly the Ge−H insertion reactivity, although the trend is not monotonic. Particularly of note are the per Ge−H rate constants showing the steady increase in values with successive ethyl substitution. Another useful comparison here is with the silylene counterpart reactions. Table 6 shows the analogous set of SiH_2 rate constants for its Si−H insertion reactions with the methylsilanes.[26] One clear feature of contrast is apparent. The effect of methyl substitution in the substrate silane actually reduces

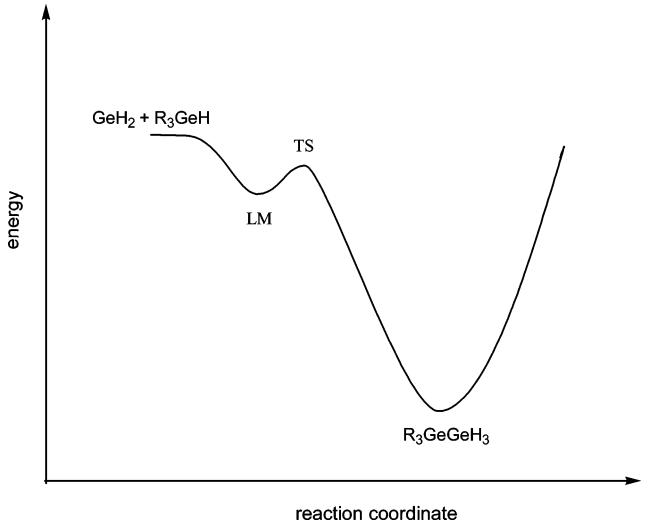

Figure 5. Generic potential energy surface for GeH_2 insertion reactions with germanes. LM is local minimum; TS is transition state.

the value of the rate constants for Si−H insertion, although the per Si−H rate constants show a small but monotonic increase with successive methyl substitution. Thus the alkyl substituent effect is much less marked for the Si−H insertion reactions (of SiH_2) than for the Ge−H insertion reactions (of GeH_2). It is also interesting to note that in the case of reaction 4, GeH_2 + Et_3GeH, the rate constant actually exceeds that for SiH_2 + Me_3SiH. The values for these rate constants are approaching the collision theory maximum (ca. 3×10^{-10} cm^3 molecule^{-1} s^{-1}), but it is unusual for GeH_2 reactions to occur faster than their SiH_2 counterparts.[15] A further comparison, which does demonstrate the lower reactivity of GeH_2 compared with SiH_2, is that of its rate constants for Si−H insertion. For GeH_2 + SiH_4, k(298 K) = 1.24×10^{-11} cm^3 molecule^{-1} s^{-1},[10] and for GeH_2 + Me_3SiH, k(298 K) = 7.64×10^{-11} cm^3 molecule^{-1} s^{-1}.[8] These are significantly less than their SiH_2 counterparts shown in Table 6. They are also significantly less than their Ge−H insertion analogues shown in Table 5, which supports the general proposition that GeH_2 will insert less readily in stronger bonds than in weaker ones. One final comparison is worth making. For GeH_2 + Me_2GeH_2, k(298 K) = 2.38×10^{-10} cm^3 molecule^{-1} s^{-1}.[11] Comparison with GeH_2 + Et_2GeH_2 (Table 5) shows that ethyl is slightly more effective than methyl in its substituent effect, and we need to exercise some caution in making some of these comparisons.

Reaction Mechanism. The insertion reactions of GeH_2, similarly to those of SiH_2, have been shown by us[6−8,10] to follow a mechanism involving an intermediate H-bonded complex, viz.

$$R_3Ge{-}H + GeH_2 \rightarrow R_3Ge{\cdots}H{\cdots}GeH_2 \rightarrow R_3GeGeH_3$$

where R is H or alkyl. The potential energy surface for such processes has the general form shown in Figure 5, in which the intermediate complex lies in a shallow well (local minimum, LM) with a secondary maximum (transition state, TS) leading to the final insertion product. In the case of GeH_2 + GeH_4, two LMs were detected, each with its own TS; furthermore, LM1 and TS2 were both sufficiently unsymmetrical to have chiral forms.[7] The most important point, however, was that we were able to show how the kinetic characteristics (magnitude of the *A* factor and negative activation energy) were dependent on the size of the secondary barrier. In the present study, the key question is how should we expect ethyl substitution to affect the height of this (or these) barriers. Although we have not carried out ab initio calculations on these reactions, we may make some inferences based on findings in the SiH_2 + methylsilane reaction systems.[26] In these latter reactions the effect of methyl substituents was to stabilize the intermediate complexes (LMs) and their accompanying transition states (TSs) by ca. 6−9 kJ mol^{-1} per Me group. If the effect for ethyl substitution on the Ge−H insertion process were of similar magnitude, we can infer that the inhibiting effect of the secondary barriers will diminish with increasing ethyl substitution, and become quite small for Et_3GeH. Since the effect of the secondary barriers on the reaction rate constant is almost negligible for the SiH_2 + SiH_4 reaction,[23] whereas it fairly large for the GeH_2 + GeH_4 reaction[7] (i.e., slowing it down), alkyl substituents should have a larger accelerating effect in the latter system, as we have found. This accelerating effect will however be temperature dependent, and as temperature increases it should become less. This is to say that the inhibiting effects of the secondary barriers become more marked at higher temperatures. The actual barrier magnitudes will determine the size of this effect, but clearly the sharper decline in rate constant values with temperature (i.e., the more negative activation energies) as ethyl substitution increases shows that secondary barriers are important for all the GeH_2 + ethylgermane reactions.

In a future publication[43] we plan to publish the results of experiments and quantum chemical calculations on the effects of methyl substituents in both germylene and substrate germane on the Ge−H insertion reaction.

Acknowledgment. We thank the following: INTAS-RFBR (Project No. IR-97-1658) and NATO (Project No. PST-.CLG975368). S.E.B, M.P.E, I.V.K., and O.M.N also thank RFBR (Project No. N 07-03-00693), the President of the Russian Federation (Presidential Program for Support of Leading Research Schools, Grant NSh-6075.2006.03), and the Russian Academy of Sciences (Programs P-09 and OX-01). R.B. thanks the Spanish DGI for support under Project No. BQU2002-03381.

References and Notes

(1) Isobe, C.; Cho, H.; Sewell, J. E. *Surf. Sci.* **1993**, *295*, 117.
(2) Du, W.; Keeling, L. A.; Greenlief, C. M. *J. Vac. Sci. Technol., A* **1994**, *12*, 2281.
(3) Newman, C. G.; Dzarnoski, J.; Ring, M. A.; O'Neal, H. E. *Int. J. Chem. Kinet.* **1980**, *12*, 661.
(4) Dzarnoski, J.; O'Neal, H. E.; Ring, M. A. *J. Am. Chem. Soc.* **1981**, *103*, 5740.
(5) Becerra, R.; Boganov, S. E.; Egorov, M. P.; Nefedov, O. M.; Walsh, R. *Chem. Phys. Lett.* **1996**, *260*, 433.
(6) Becerra, R.; Boganov, S. E.; Egorov, M. P.; Nefedov, O. M.; Walsh, R. *Mendeleev Commun.* **1997**, 87.
(7) Becerra, R.; Boganov, S. E.; Egorov, M. P.; Faustov, V. I.; Nefedov, O. M.; Walsh, R. *J. Am. Chem. Soc.* **1998**, *120*, 12657.
(8) Becerra, R.; Walsh, R. *Phys. Chem. Chem. Phys.* **1999**, *1*, 5301.
(9) Becerra, R.; Boganov, S. E.; Egorov, M. P.; Faustov, V. I.; Nefedov, O. M.; Walsh, R. *Can. J. Chem.* **2000**, *78*, 1428.
(10) Becerra, R.; Boganov, S. E.; Egorov, M. P.; Faustov, V. I.; Nefedov, O. M.; Walsh, R. *Phys. Chem. Chem. Phys.* **2001**, *3*, 184.
(11) Becerra, R.; Egorov, M. P.; Krylova, I. V.; Nefedov, O. M.; Walsh, R. *Chem. Phys. Lett.* **2002**, *351*, 47.
(12) Becerra, R.; Boganov, S. E.; Egorov, M. P.; Faustov, V. I.; Promyslov, V. M.; Nefedov, O. M.; Walsh, R. *Phys. Chem. Chem. Phys.* **2002**, *4*, 5079.
(13) Becerra, R.; Walsh, R. *Phys. Chem. Chem. Phys.* **2002**, *4*, 6001.
(14) Becerra, R.; Boganov, S. E.; Egorov, M. P.; Faustov, V. I.; Krylova, I. V.; Nefedov, O. M.; Promyslov, V. M.; Walsh, R. *Phys. Chem. Chem. Phys.* **2004**, *6*, 3370.
(15) Boganov, S. E.; Egorov, M. P.; Faustov, V. I.; Krylova, I. V.; Nefedov, O. M.; Becerra, R.; Walsh, R. *Russ. Chem. Bull. Int. Ed.* **2005**, *54*, 483.
(16) Alexander, U. N.; Trout, N. A.; King, K. D.; Lawrance, W. D. *Chem. Phys. Lett.* **1999**, *299*, 291.
(17) Alexander, U. N.; King, K. D.; Lawrance, W. D. *Chem. Phys. Lett.* **2000**, *319*, 529.

(18) Alexander, U. N.; King, K. D.; Lawrance, W. D. *Phys. Chem. Chem. Phys.* **2003**, *5*, 1557.
(19) Becerra, R.; Walsh, R. Kinetics & mechanisms of silylene reactions: A prototype for gas-phase acid/base chemistry. In *Research in Chemical Kinetics*; Compton, R. G., Hancock, G., Eds.; Elsevier: Amsterdam, 1995; Vol. 3, p 263.
(20) Jasinski, J. M.; Becerra, R.; Walsh, R. *Chem. Rev.* **1995**, *95*, 1203.
(21) Baggott, J. E.; Frey, H. M.; Lightfoot, P. D.; Walsh, R.; Watts, I. M. *J. Chem. Soc., Faraday Trans.* **1990**, *86*, 27.
(22) Becerra, R.; Frey, H. M.; Mason, B. P.; Walsh, R.; Gordon, M. S. *J. Am. Chem. Soc.* **1992**, *114*, 2751.
(23) Becerra, R.; Frey, H. M.; Mason, B. P.; Walsh, R.; Gordon, M. S. *J. Chem. Soc., Faraday Trans.* **1995**, *91*, 2723.
(24) Becerra, R.; Frey, H. M.; Mason, B. P.; Walsh, R. *J. Organomet. Chem.* **1996**, *521*, 343.
(25) Becerra, R.; Boganov, S.; Walsh, R. *J. Chem. Soc., Faraday Trans.* **1998**, *94*, 3569.
(26) Becerra, R.; Carpenter, I. M.; Gordon, M. S.; Roskop, L.; Walsh, R. Submitted for publication in *Phys. Chem. Chem. Phys.* **2006**.
(27) Campargue, A.; Escribano, R. *Chem. Phys. Lett.* **1999**, *315*, 397.
(28) (a) *Inorganic Synthesis*; Jolly, W. L., Ed.; McGraw-Hill: New York, 1968; p 176. (b) Zueva, G. Ya.; Pogorelov, A. G.; Pisarenko, V. I.; Snegova, A. D.; Ponomarenko, V. A. *Neorg. Mater.* **1966**, *2* (8), 1359 (in Russian).
(29) Mironov, V. M.; Kravchenko, A. L. *Izv. Acad. Nauk. USSR* **1965**, 1026 (in Russian).
(30) Tabern, D. L.; Orndorff, W. R.; Dennis, L. M. *J. Am. Chem. Soc.* **1925**, *47*, 2043.
(31) Holbrook, K. A.; Pilling, M. J.; Robertson, S. H. *Unimolecular Reactions*, 2nd ed.; Wiley: Chichester, 1996.
(32) Vanderwielen, A. J.; Ring, M. A.; O'Neal, H. E. *J. Am. Chem. Soc.* **1975**, *97*, 993.
(33) O'Neal, H. E.; Ring, M. A.; Richardson, W. H.; Liciardi, G. F. *Organometallics* **1989**, *8*, 1968.
(34) Urban, J.; Schreiner, P. R.; Vacek, G.; Schleyer, P. v. R.; Huang, J. Q.; Leszczynski, J. *Chem. Phys. Lett.* **1997**, *264*, 441.
(35) Benson, S. W. *Thermochemical Kinetics*, 2nd ed.; Wiley: New York, 1976.
(36) Troe, J. *J. Chem. Phys.* **1977**, *66*, 4758.
(37) Reid, R. C.; Prausnitz, J. M.; Poling, B. E. *The properties of gases and liquids*, 4th ed.; McGraw-Hill: New York, 1988.
(38) Hippler, H.; Troe, J. In *Advances in Gas Phase Photochemistry and Kinetics*; Ashfold, M. N. R., Baggott, J. E., Eds.; Royal Society of Chemistry: London, 1989; Vol. 2, Chapter 5, p 209.
(39) Cvetanović, R. J. Mercury Photosensitized Reactions. In *Progress in Reaction Kinetics*; Porter, G., Ed.; Pergamon: London, 1964; Vol. 2, Chapter 2, p 41.
(40) Gaspar, P. P.; Levy, C. A.; Frost, J. J.; Bock, S. A. *J. Am. Chem. Soc.* **1969**, *91*, 1573.
(41) Estacio, P.; Sefcik, M. D.; Chan, E. K.; Ring, M. A. *Inorg. Chem.* **1970**, *9*, 1068.
(42) Sefcik, M. D.; Ring, M. A. *J. Organomet. Chem.* **1973**, *59*, 167.
(43) Becerra, R.; Boganov, S. E.; Egorov, M. P.; Faustov, V. I.; Krylova, I. V.; Nefedov, O. M.; Promyslov, V. M.; Walsh, R. Manuscript in preparation.